Research article

Simon Mahler, Yaniv Eliezer, Hasan Yılmaz, Asher A. Friesem, Nir Davidson and Hui Cao*

Fast laser speckle suppression with an intracavity diffuser

https://doi.org/10.1515/nanoph-2020-0390
Received July 10, 2020; accepted September 2, 2020;
published online September 22, 2020

Abstract: Fast speckle suppression is crucial for time-resolved full-field imaging with laser illumination. Here, we introduce a method to accelerate the spatial decoherence of laser emission, achieving speckle suppression in the nanosecond integration time scale. The method relies on the insertion of an intracavity phase diffuser into a degenerate cavity laser to break the frequency degeneracy of transverse modes and broaden the lasing spectrum. The ultrafast decoherence of laser emission results in the reduction of speckle contrast to 3% in less than 1 ns.

Keywords: optical coherence; optics and lasers; laser dynamics; speckle.

1 Introduction

Conventional lasers have a high degree of spatial coherence, manifesting coherent artifacts and cross-talk. One prominent example is speckle noise, which is detrimental to laser applications such as imaging, display, material processing, photolithography, optical trapping and more [1]. Several techniques have been developed to suppress speckle noise by incoherently integrating many uncorrelated speckle realizations, e.g., by using a moving diffuser or aperture [2–9]. Typically, these methods are effective only at long integration times of a millisecond or longer.

Fast speckle suppression is essential for time-resolved imaging of moving targets or transient phenomena [10–12]. It can be achieved by using multimode lasers with low and tunable spatial coherence [13–19]. The decoherence time of such lasers, critical for fast speckle suppression in short integration times, is determined by the frequency spacing and linewidth of the individual lasing modes, as well as the total width of the emission spectrum $\Delta\Omega$ [20]. Let us consider N transverse modes lasing simultaneously and assume that the linewidth of each individual transverse mode is smaller than the typical frequency spacing $\Delta\omega_t$ of neighboring modes. Only when the integration time τ exceeds $1/\Delta\Omega$, the modal decoherence starts. Once τ exceeds $1/\Delta\omega_t$, the N lasing modes become mutually incoherent and the speckle contrast C is reduced to $1/\sqrt{N}$. Therefore, broadening the laser emission spectrum and increasing the frequency spacing between the transverse modes accelerates speckle suppression, as demonstrated recently with a broad-area semiconductor laser [19].

To reach low spatial coherence, a large number of transverse modes must lase simultaneously. This requires the modes to have a similar loss or quality factor, which can be achieved with a degenerate cavity laser (DCL) [21]. The DCL self-imaging configuration ensures that all transverse modes have an almost identical (degenerate) quality factor. Experimentally, it has been shown that $N \approx 320{,}000$ transverse modes can lase simultaneously and independently in a solid-state DCL [22]. But the transverse modes are also nearly degenerate in frequency, which implies a longer decoherence (integration) time. In the short nanosecond time scale, the longitudinal modes play a critical role in spatial coherence reduction [11]. In particular, the spatiotemporal dynamics of a DCL having M longitudinal modes reduces the speckle contrast to $1/\sqrt{M}$. However, since the number of longitudinal modes is typically far less than the number of transverse modes ($M \ll N$), the speckle contrast reduction at short time scales is limited.

In this work, we develop a simple and robust method for ultrafast speckle suppression. We accelerate the spatial decoherence of a DCL by inserting a phase diffuser

Simon Mahler and Yaniv Eliezer: These authors contributed equally to this work.

***Corresponding author: Hui Cao**, Department of Applied Physics, Yale University, New Haven, Connecticut 06520, USA,
E-mail: hui.cao@yale.edu
Simon Mahler, Asher A. Friesem and Nir Davidson, Department of Physics of Complex Systems, Weizmann Institute of Science, Rehovot 761001, Israel. https://orcid.org/0000-0002-9761-445X (S. Mahler)
Yaniv Eliezer and Hasan Yılmaz, Department of Applied Physics, Yale University, New Haven, Connecticut 06520, USA. https://orcid.org/0000-0002-6203-5044 (Y. Eliezer). https://orcid.org/0000-0003-1889-3516 (H. Yılmaz)

(random phase plate) into the cavity. The intracavity phase diffuser lifts the frequency degeneracy of transverse modes and broadens the lasing spectrum. Simultaneously, a large number of transverse modes manage to lase because of their high quality factors. The speckle contrast is reduced to 3% (below human perception level [23]) in less than 1 ns. The lasing threshold is slightly increased (5–10%) with the intracavity phase diffuser, and the output power is reduced by merely 15% over a wide range of pump levels. This work provides a simple and robust method for ultrafast speckle suppression.

2 Degenerate cavity laser configurations

Figure 1 schematically presents several different DCL configurations (details are given in Section 5.1). Figure 1A shows the basic DCL in a self-imaging condition [22]. It comprises of a high-reflectivity flat back mirror, a Nd:YAG gain medium optically pumped by a flash lamp, two spherical lenses of focal lengths f in a $4f$ telescope configuration and an output coupler. We calculate the transverse mode structure (see Section 5.2 for details) and plot the histogram of the frequency differences between the nth order transverse mode ω_n and the fundamental mode ω_0. The difference $\omega_n - \omega_0$ is normalized by the free spectral range (FSR = $\Delta\omega_l$), which is the frequency spacing of longitudinal mode groups. The results shown in the center panel indicate that all the transverse modes in a perfect DCL are exactly degenerate in frequency. The quality factor as a function of the transverse mode index in the right panel exhibits a uniform distribution of high quality factors, indicating that all the transverse modes have an exactly identical (degenerate) quality factor. In this ideal case, despite the fact that many transverse modes are expected to lase, the spectral degeneracy slows down the spatial decoherence. Only when the photodetection integration time exceeds the coherence time given by the inverse of spectral linewidth of individual lasing modes, the degenerate modes become mutually incoherent and the speckle contrast decreases. Note that in practice such an ideal DCL cannot be realized due to the presence of misalignment errors, thermal effects and optical aberrations [24]. Therefore, the transverse lasing modes have slightly different frequencies, which in turn shorten the time of decoherence [22].

In order to accelerate the spatial decoherence, the frequency spacing of the transverse modes has to be increased. Namely, the frequency degeneracy of the modes has to be broken. A conventional method for breaking the frequency degeneracy is detuning the cavity, e.g., translating the output coupler in the longitudinal (z) axis of the cavity, as shown in the configuration of Figure 1B. With a sufficient longitudinal displacement Δz, i.e., $\Delta z = 0.04f$ for our cavity geometry, the frequency spacings of the transverse modes are extended to the entire FSR (center panel). However, the degeneracy in quality factors is also lifted, and many modes suffer a severe quality factor degradation (right panel). Therefore, the number of lasing modes will be significantly reduced, resulting in an effectively higher speckle contrast.

In order to break the frequency degeneracy and increase the frequency spacings of the transverse modes, while minimizing their quality factor degradation, we explore a different approach, where we insert a static intracavity phase diffuser into the DCL, as shown in Figure 1C. The phase diffuser is placed next to the output coupler in order to maintain the self-imaging condition of the cavity. More details are given in Section 5.1. The intracavity phase diffuser is a computer-generated random phase plate made of glass. It introduces an optical phase delay that varies randomly from $-\pi$ to π on a length scale of $\approx$200 μm (see Section 5.1). The center panel of Figure 1C shows that the transverse modes are spread over the entire FSR of the DCL, increasing the frequency spacings between them. In contrary to the misaligned cavity case, many transverse modes experience minor quality factor degradation. As a result, a large number of transverse modes are expected to lase over a wide spectrum of frequencies, accelerating the speckle suppression process.

3 Ultrafast speckle suppression

To demonstrate the efficiency of our method, we experimentally measure the speckle contrast for integration times in the range of 10^{-10} to 10^{-4} s. The output beam of the DCL is incident onto a thin diffuser placed outside the laser cavity. Then, the speckle intensity is measured by an InGaAs photodiode of 15 GHz bandwidth and an oscilloscope of 4 GHz bandwidth. See Section 5.1 for a detailed description of the experimental setup and the measurement scheme. Figure 2A shows the measured speckle contrast as a function of the photodetector's integration time without and with an intracavity phase diffuser, at the pump power of three times the lasing threshold. By measuring the speckle contrast over many time windows of an equal length, we compute the mean contrast value and estimate the uncertainty that is shown by the shaded area. The lasing pulse is ~100 μs long. To avoid the transient oscillations at the

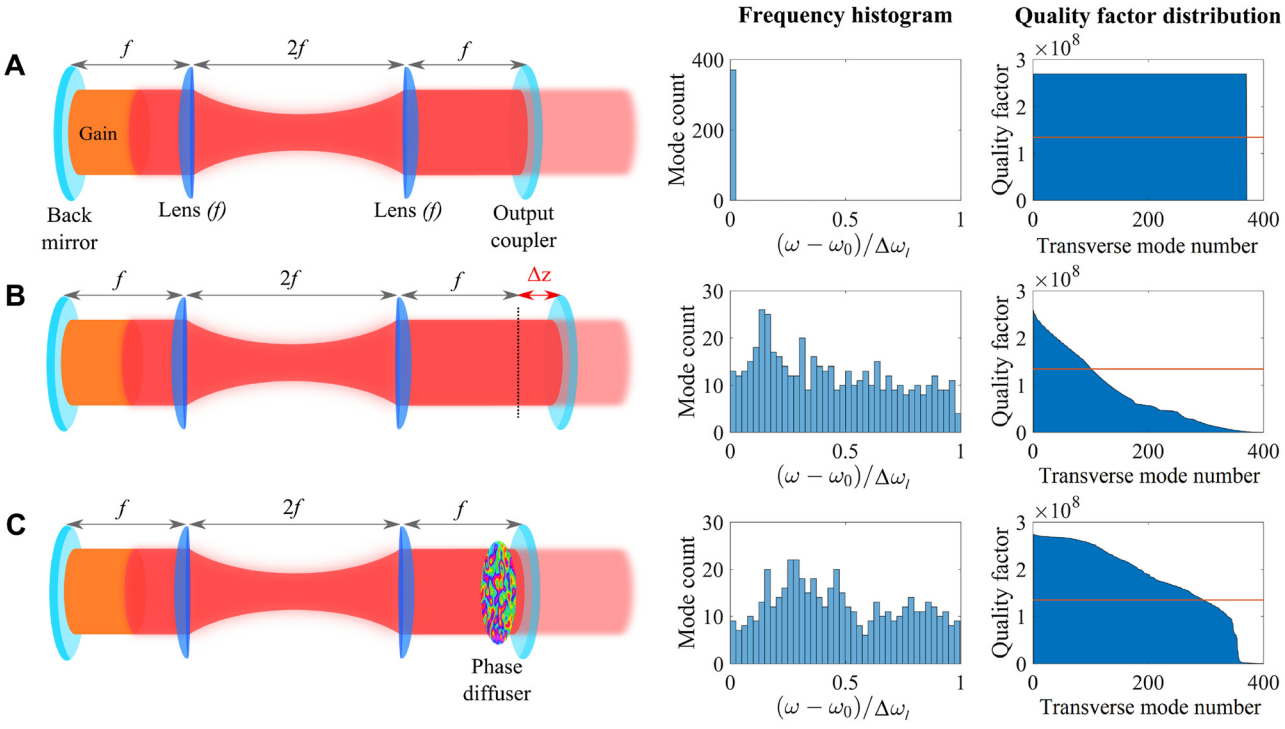

Figure 1: Degenerate cavity laser (DCL) configurations. (A) An ideal DCL with a total length of $4f$. (B) A misaligned DCL. The output coupler is longitudinally translated by Δz along the cavity axis z, with a total cavity length of $4f + \Delta z$. (C) A DCL with an intracavity phase diffuser placed next to the output coupler. The left column contains a sketch of each cavity configuration, the middle column shows the histogram of the frequency differences between the transverse modes and the fundamental one within one longitudinal mode group normalized by the free spectral range: $(\omega - \omega_0)/\Delta\omega_l$ and the right column plots the quality factor versus transverse mode index. The red horizontal line marks half of the maximum quality factor as a reference. The ideal DCL has a large number of high-quality transverse modes, all with the same frequency (both frequency and quality factor degeneracies). The longitudinally misaligned DCL has many modes with different frequencies but also has a relatively small number of transverse modes with high quality factors (no degeneracies). The DCL with a phase diffuser has a relatively large number of high-quality transverse modes with enhanced frequency differences, enabling ultrafast speckle suppression.

beginning of the lasing pulse, we analyze the emission after the laser reaches a quasi steady state. For the effects of lasing transients, see Supplementary material S1. Experimental data with a lower pump power are also presented in Supplementary material S2.

With the intracavity phase diffuser, the speckle contrast at short integration times (between 10^{-10} and 10^{-7} s) is significantly lower than that without the intracavity phase diffuser. Even when the integration time is as short as 10^{-9} s, the speckle contrast is already reduced to 3%. To understand this remarkable result, we numerically calculate the field evolution in a passive cavity with a simplified (1+1)D model. Nonlinear interactions of the lasing modes through the gain medium are neglected (see Section 5.2 for details about the numerical model). The calculated speckle contrast is plotted as a function of integration time τ in Figure 2B. When τ is shorter than the inverse of the emission spectrum width $1/\Delta\Omega$, all lasing modes within $\Delta\Omega$ are mutually coherent with each other.

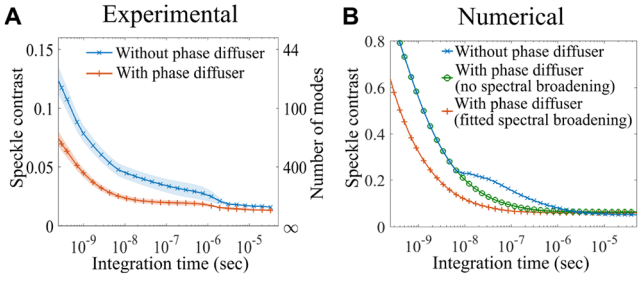

Figure 2: Speckle contrast as a function of the photodetector's integration time measured for the DCL without and with an intracavity phase diffuser. The pump power is roughly three times the lasing threshold ($P \approx 3P_{th}$). (A) Experimental data. (B) Numerical results. Experimentally, the intracavity phase diffuser introduces a significant reduction in speckle contrast for integration times τ less than 10^{-6} s. Numerically, the reduction of speckle contrast by the intracavity phase diffuser is seen for 10^{-8} s $< \tau < 10^{-6}$ s without spectral broadening (green). Further spectral broadening by the intracavity diffuser causes additional speckle reduction in shorter time scales $\tau < 10^{-8}$ s (red).

The interference of their fields scattered by the external diffuser produces a speckle pattern of unity contrast ($C \approx 1$).

Once $\tau > 1/\Delta\Omega$, the lasing modes of frequency spacing larger than $1/\tau$ decohere with respect to each other, and the intensity sum of their scattered light reduces the speckle contrast. With increasing τ, more lasing modes become mutually incoherent, and the speckle contrast continues to drop. In a slightly imperfect DCL without the phase diffuser, the longitudinal mode spacing $\Delta\omega_l$ is much larger than the transverse mode spacing $\Delta\omega_t$. Once τ exceeds $1/\Delta\omega_l \sim 10^{-8}$ s, different longitudinal modal groups are mutually incoherent, but the transverse modes within each longitudinal modal group remain coherent till τ reaches $1/\Delta\omega_t \sim 10^{-6}$ s. Thus, the speckle contrast reduction is greatly slowed down in the time interval between 10^{-8} and 10^{-6} s. Once τ exceeds 10^{-6} s, the decoherence of the transverse modes leads to a further reduction of speckle contrast. See the study by Chriki et al. [11] for a comprehensive theory.

With an intracavity phase diffuser in the DCL, the gap between $\Delta\omega_l$ and $\Delta\omega_t$ diminishes as the intracavity phase diffuser introduces different phase delays (frequency shifts) to individual transverse modes (as depicted in Figure 1C). Meanwhile, the intracavity phase diffuser causes a relatively small reduction in the quality factor of many transverse modes. Thus, a large number of transverse modes can still lase and their frequency detuning accelerates the spatial decoherence. In the time interval of 10^{-8} to 10^{-6} s, the speckle contrast continues to decrease due to the decoherence of the transverse modes within one FSR.

To verify this explanation, we compare the power spectrum of emission intensity of the DCL with the intracavity phase diffuser to that without it. The power spectrum is obtained by Fourier transforming the time intensity signal of the emission. Figure 3 shows the measured and simulated power spectra, which reflect the frequency beating of the lasing modes. Without the intracavity phase diffuser (top row), the power spectrum features narrow distributions peaked at the harmonics of FSR = $c/(2L) \approx 128$ MHz, where c is the speed of light, and $L = 117$ cm is the total optical length of the DCL. The narrow distributions centered at the harmonics of the FSR reveal a slight breaking of frequency degeneracy of the transverse modes, due to the inherent imperfections of the cavity. With the intracavity phase diffuser (bottom row), the power spectrum of emission intensity features many narrow peaks in between the harmonics of the FSR. As the transverse modes move further away from the frequency degeneracy, their frequency differences, which determine their beat frequencies, increase. Nevertheless, the longitudinal mode spacing is unchanged; thus, the peaks at the harmonics of the FSR remain in the power spectrum but appear narrower than that without the intracavity phase diffuser. The changes in the power spectrum indicate a frequency broadening of spatiotemporal modes by the intracavity phase diffuser. An ensemble of mutually incoherent lasing modes separated by frequency spacings in the range of ~1 to ~128 MHz leads to a faster decoherence rate on the time scale of ~10^{-8} to ~10^{-6} s. This observation is consistent with the behavior shown in Figure 2.

Surprisingly, the intracavity phase diffuser causes a significant speckle contrast reduction even when the integration time is shorter than 10^{-8} s, as seen in Figure 2A. Note that this behavior is not captured in the simulation (Figure 2B, green curve). To explain this effect, we analyze the entire experimentally measured power spectra [25]. The results are presented in Figure 4 both (A) without and (B) with the phase diffuser in the DCL.

Without the intracavity phase diffuser, the power spectrum envelope decays with increasing frequency. With the intracavity phase diffuser, the power spectrum exhibits an essentially constant envelope over the entire power detection range of 5 GHz. This difference indicates that the intracavity phase diffuser facilitates lasing in a broader frequency range. With the intracavity phase diffuser, the mutually incoherent lasing modes of frequency spacing well above 1 GHz accelerate the speckle reduction in the subnanosecond time scale. Due to the large number of lasing modes in the DCL, it is extremely difficult to simulate their nonlinear interactions with the gain material. Our numerical model does not account for spatial hole burning and mode

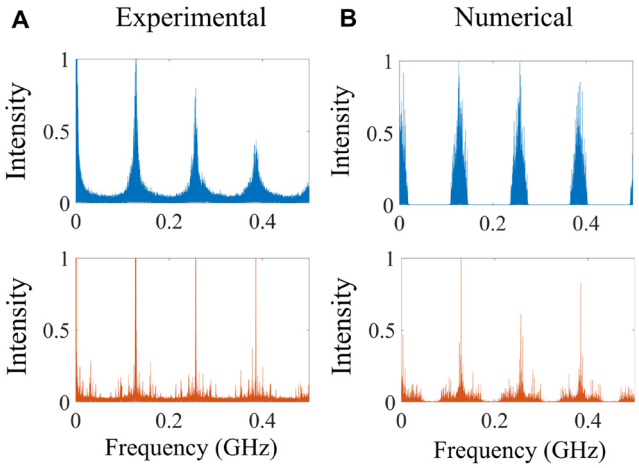

Figure 3: Power spectra of the DCL's emission intensity without (top row) and with (bottom row) the phase diffuser. (A) Experimental data. (B) Numerical results. The intracavity phase diffuser broadens the radiofrequency distribution in each FSR unit, increasing the frequency spacing of the transverse modes and leading to faster spatial decoherence and speckle suppression.

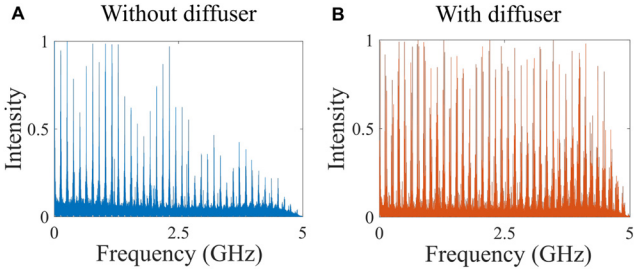

Figure 4: Experimentally measured full-scale power spectrum of emission intensity of the degenerate cavity laser (A) without and (B) with the intracavity phase diffuser. The power spectrum envelope decreases with frequency in (A) and remains nearly constant in (B), indicating that the intracavity phase diffuser enhances lasing in a broader spectral range and accelerates speckle suppression within 1 ns integration time.

competition for gain and thus cannot predict the lasing spectrum broadening induced by the intracavity diffuser. Therefore, the difference between the experimental and the numerical results in the ultrashort time regime is attributed to the absence of nonlinear lasing dynamics in the numerical model. Namely, the intracavity phase diffuser reduces mode competition for gain, allowing modes with wider frequency differences to lase simultaneously.

To complete this observation, we incorporate the diffuser-induced broadening of the lasing spectrum into the numerical model and calculate the spectral contrast as shown by the red curve in Figure 2B. Lasing with more longitudinal modal groups results in a more significant reduction of the speckle contrast at short integration times, in agreement to the experimental data in Figure 2A. This agreement confirms two distinct mechanisms for speckle contrast reduction by the intracavity diffuser. One is the increase of frequency spacing of the transverse modes within each longitudinal modal group, and the other is the broadening of the entire lasing spectrum and an increase in the total number of longitudinal modal groups that can lase. The former mechanism results in speckle reduction in the integration time range of 10^{-8} to 10^{-6} s, while the latter is responsible for speckle reduction in the range of 10^{-10} to 10^{-8} s.

Finally, we measure the total output power of the DCL without and with the intracavity phase diffuser. The lasing threshold is increased by 5–10% after the diffuser is inserted into the DCL. As shown in Section 5.4, the output power is reduced by about 15% over a wide range of pump levels from 1.2 times to 3.3 times the lasing threshold power.

4 Conclusion

In conclusion, we accelerate the spatial decoherence of a degenerate cavity laser (DCL) with an intracavity phase diffuser. In less than 1 ns, the speckle contrast is already reduced to 3%, below the human perception level. Such a light source, together with a time-gated camera, can be used for time-resolved full-field imaging of transient phenomena such as the dynamics of material processing [10] and tracking of moving targets [11, 22]. Our approach is general and will work more efficiently in terms of speckle reduction for compact multimode lasers that have a smaller number of lasing modes and a higher speckle contrast than our DCL. We plan to extend this work by further investigating how the intracavity phase diffuser modifies the nonlinear modal interactions and the spatiotemporal dynamics of a DCL [26].

5 Methods

5.1 Detailed experimental setup

Our experimental setup, shown in Figure 5, consists of two parts: (i) a DCL with a static intracavity phase diffuser and (ii) an imaging system to generate speckle with an external diffuser and to measure speckle contrast [11]. The DCL comprises a flat back mirror with 95% reflectivity, a Nd:YAG crystal rod of 10.9 cm length and 0.95 cm diameter, two spherical lenses of 5.08 cm diameter and f = 25 cm focal length and an output coupler with 80% reflectivity. Adjacent to the output coupler, the phase diffuser is placed inside the cavity.

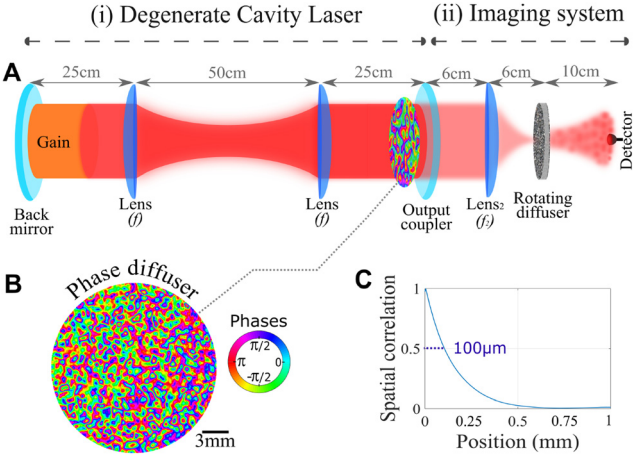

Figure 5: Experimental configuration for the time-resolved speckle intensity measurement. (A) Sketch of (i) a degenerate cavity laser (DCL) with an intracavity phase diffuser and (ii) an imaging system with an external diffuser for generating speckle and a photodetector for measuring the speckle intensity as a function of time. (B) The two-dimensional phase profile of the intracavity phase diffuser, measured by a home-built optical interferometer. (C) Cross section of the two-dimensional autocorrelation function of the phase profile shown in (B), its width gives the typical length scale over which the phase varies.

Lasing occurs at the wavelength of 1064 nm with optical pumping. The output beam is focused by a lens with a diameter of 2.54 cm and a focal length of f_2 = 6 cm onto a thin diffuser with a 10° angular spread of the transmitted light. A photodetector with a 15 GHz bandwidth and 30 μm diameter is placed at a distance of 10 cm from the diffuser and records the scattered light intensity within a single speckle grain in time. We rotate the diffuser and repeat the time intensity trace measurement of a different speckle grain. In total, 100 time intensity traces are recorded.

The intracavity phase diffuser (Figure 5B) is a computer-generated surface relief random phase plate of diameter 5.08 cm and thickness 2.3 mm. The angular spread of the transmitted light is 0.3°. The two-dimensional phase profile across the phase diffuser is measured with a home-built optical interferometer. The phase randomly varies in 16 equal steps between $-\pi$ to π with a uniform probability density. From the measured phase profile, we compute the spatial correlation function, as shown in Figure 5C. Its half width at half maximum is 100 μm. The spatial correlation length is 200 μm, in agreement with the angular spread of the scattered light from the phase diffuser.

In the time-resolved speckle measurement, we use an InGaAs photodiode with 15 GHz bandwidth (Electro-Optics ET-3500). It is connected via a radiofrequency coaxial cable to a Keysight DSO9404A oscilloscope of 4 GHz bandwidth and up to 20 GS/s sampling rate (giga sample per second). The effective bandwidth of our detection system is thus limited to 4 GHz by the oscilloscope.

5.2 Numerical simulation

We simulate continuous wave propagation in a passive degenerate cavity with and without the intracavity phase diffuser. The cavity length and width are identical to those of the DCL in our experiment, except that the cross section is one dimensional in order to shorten the computation time. Without the intracavity phase diffuser, the field evolution matrix of a single round trip in the cavity is given as follows:

$$M^{wo} = M_B \cdot M_\epsilon \cdot M_F \tag{1}$$

where M_F is the field propagation matrix from the back mirror to the output coupler and M_B from the output coupler to the back mirror and M_ϵ represents a small axial misalignment of the DCL [24]. With the intracavity phase diffuser placed next to the output coupler, the field evolution matrix of a single round trip becomes:

$$M^{w} = M_B \cdot M_\epsilon \cdot M_{PD} \cdot M_F, \tag{2}$$

where M_{PD} represents the phase delay of the field induced by the phase diffuser for one round trip in the cavity. To construct M_{PD} in our simulations, we use the spatial distribution of the phase delay taken from the measured profile in Figure 5B.

The matrices M^{wo} and M^{w} are diagonalized to obtain the eigenmodes of the cavity without and with the intracavity phase diffuser. A subset of the eigenmodes has high quality factors (low losses). Hence, they have low lasing threshold and correspond to the lasing modes. The total field in the cavity can be expressed as a sum of these modes:

$$E(x,t) = \sum_{m=-M}^{M} \sum_{n=1}^{N} \alpha_{m,n} \psi_n(x) e^{i\left[\omega_{m,n} t + \phi_{m,n}(t)\right]}, \tag{3}$$

where $\alpha_{m,n}$ and $\omega_{m,n}$ denote the amplitude and frequency of a mode, respectively, with a longitudinal index m and a transverse index n and $\psi_n(x)$ represents the transverse field profile for the nth eigenmode. The phase $\phi_{m,n}(t)$ fluctuates randomly in time to simulate the spontaneous emission–induced phase diffusion that leads to spectral broadening [27]. The total number of transverse modes is N, and the number of longitudinal modes is $2M$.

The optical gain spectrum is approximated as a Lorentzian function centered at ω_0 with a full width at half maximum of 32 GHz. All lasing modes are within the gain spectrum and their frequencies can be written as $\omega_{m,n} = \omega_0 + m\Delta\omega_l + \omega_n$, where $\Delta\omega_l$ is the longitudinal mode spacing (FSR), $m = \{-M, \ldots +M\}$, M = 16 and ω_n is the transverse mode frequency. The total number of time steps in the simulation of field evolution is 10^6, each step has the duration of 0.1 ns. The power spectrum is calculated by Fourier transforming the time trace of the intensity $|E(x,t)|^2$.

To generate an intensity speckle, we simulate the field propagation from the output coupler of the degenerate cavity to the external diffuser and then from the diffuser to the far field. The field intensity at the far field is used to compute the speckle contrast as a function of the integration time (see Methods 5.3).

5.3 Measurement of speckle contrast

We use the experimental setup in Figure 5A to measure the time-resolved intensity of a single speckle grain behind a diffuser that is placed outside of the DCL. Using the detection device, we record the intensity as a function of time with and without the phase diffuser inside the DCL. The time trace of the intensity is recorded at 100 spatial locations $\vec{r}_i = (x_i, y_i)$, where i = 1…100, by rotating the external diffuser by 3.6° for each realization. From the 100 intensity traces, we calculate the speckle contrast C as a function of the integration time τ. First, the total time window T is divided into $J = T/\tau$ intervals. For the jth interval, the intensity is integrated in time: $I_j(\vec{r}_i, \tau) = \int_{j\tau}^{(j+1)\tau} I(\vec{r}_i, t)\, dt$, where $I(\vec{r}_i, t)$ is the time trace of intensity measured at location $\vec{r}_i$. Then, the speckle contrast is calculated for the integration time of τ for the jth interval:

$$C_j(\tau) = \frac{\sigma_j(\tau)}{\mu_j(\tau)}, \tag{4}$$

where $\sigma_j(\tau) = \sqrt{\langle I_j^2(\vec{r}_i, \tau)\rangle_i - \langle I_j(\vec{r}_i, \tau)\rangle_i^2}$ is the standard deviation and $\mu_j(\tau) = \langle I_j(\vec{r}_i, \tau)\rangle_i$ is the mean intensity over i = 1…100 spatial locations. Finally, we compute the mean speckle contrast over all time intervals of length τ: $C(\tau) = \langle C_j(\tau)\rangle_j$. The uncertainty of $C(\tau)$ is estimated from the standard deviation: $\sigma_C(\tau) = \sqrt{\langle C_j(\tau)^2\rangle_j - C(\tau)^2}$. Repeating this method, we compute the speckle contrast for different integration times τ in the range from 10^{-10} to 10^{-4} s [11].

5.4 Total output power of the DCL configurations

We experimentally measure the total output power of the DCL without and with the intracavity phase diffuser. As shown in Figure 6A, the total output power with the intracavity phase diffuser is slightly lower than that without it. In Figure 6B, we plot their ratio, which is about 0.85 for all the pump levels. Thus, the intracavity phase diffuser causes a power reduction of about 15%. The lasing threshold is also slightly increased (5–10%) with the intracavity phase diffuser.

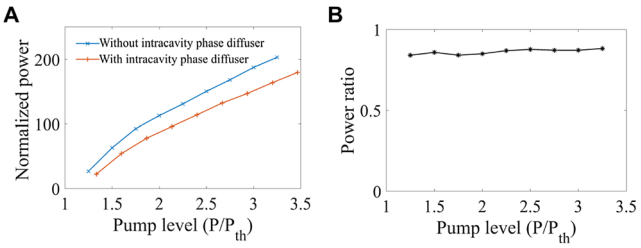

Figure 6: Total output power of the degenerate cavity laser (DCL) with and without the intracavity phase diffuser. (A) The measured output power normalized by the value just above the lasing threshold as a function of the pump power normalized by the threshold value P_{th}. (B) Ratio of the output power from the DCL with the intracavity phase diffuser to that without it. The intracavity phase diffuser reduces the output power by 15% at all pump levels.

Acknowledgments: The authors thank Arnaud Courvoisier and Ronen Chriki for their advice and help in the measurements. This work is partially funded by the US-Israel Binational Science Foundation (BSF) under grant no. 2015509. The work performed at Yale is supported partly by the US Air Force Office of Scientific Research under Grant No. FA 9550-20-1-0129, and the authors acknowledge the computational resources provided by the Yale High Performance Computing Cluster (Yale HPC). The research done at Weizmann is supported by the Israel Science Foundation.

Author contribution: All the authors have accepted responsibility for the entire content of this submitted manuscript and approved submission.

Research funding: This work is partially funded by the US-Israel Binational Science Foundation (BSF) under grant no. 2015509. The work performed at Yale is supported partly by the US Air Force Office of Scientific Research under Grant No. FA 9550-20-1-0129.

Conflict of interest statement: The authors declare no conflicts of interest regarding this article.

References

[1] J. W. Goodman, *Speckle Phenomena in Optics: Theory and Applications*, Englewood, Colorado, Roberts and Company, 2010.

[2] K. V. Chellappan, E. Erden, and H. Urey, "Laser-based displays: a review," *Appl. Opt.*, vol. 49, no. 25, pp. F79–F98, Sep 2010.

[3] S. Lowenthal and D. Joyeux, "Speckle removal by a slowly moving diffuser associated with a motionless diffuser," *J. Opt. Soc. Am.*, vol. 61, no. 7, pp. 847–851, Jul 1971.

[4] T. S. McKechnie, "Reduction of speckle by a moving aperture – first order statistics," *Opt. Commun.*, vol. 13, no. 1, pp. 35–39, 1975.

[5] C. Saloma, S. Kawata, and S. Minami, "Speckle reduction by wavelength and space diversity using a semiconductor laser," *Appl. Opt.*, vol. 29, no. 6, pp. 741–742, Feb 1990.

[6] Y. Kuratomi, K. Sekiya, H. Satoh, et al., "Speckle reduction mechanism in laser rear projection displays using a small moving diffuser," *J. Opt. Soc. Am. A*, vol. 27, no. 8, pp. 1812–1817, Aug 2010.

[7] L. Waller, G. Situ, and J. W. Fleischer, "Phase-space measurement and coherence synthesis of optical beams," *Nat. Photonics*, vol. 6, no. 7, pp. 474–479, 2012.

[8] T.-T.-K. Tran, Ø. Svensen, X. Chen, and M. Nadeem Akram, "Speckle reduction in laser projection displays through angle and wavelength diversity," *Appl. Opt.*, vol. 55, no. 6, pp. 1267–1274, Feb 2016.

[9] M. Nadeem Akram and X. Chen, "Speckle reduction methods in laser-based picture projectors," *Opt. Rev.*, vol. 23, no. 1, pp. 108–120, 2016.

[10] A. Mermillod-Blondin, H. Mentzel, and A. Rosenfeld, "Time-resolved microscopy with random lasers," *Opt. Lett.*, vol. 38, no. 20, pp. 4112–4115, Oct 2013.

[11] C. Ronen, S. Mahler, C. Tradonsky, V. Pal, A. A. Friesem, and N. Davidson, "Spatiotemporal supermodes: rapid reduction of spatial coherence in highly multimode lasers," *Phys. Rev. A*, vol. 98, p. 023812, Aug 2018.

[12] S. Knitter, C. Liu, B. Redding, M. K. Khokha, M. A. Choma, and C. Hui, "Coherence switching of a degenerate vecsel for multimodality imaging," *Optica*, vol. 3, no. 4, pp. 403–406, Apr 2016.

[13] B. Redding, M. A. Choma, and H. Cao, "Spatial coherence of random laser emission," *Opt. Lett.*, vol. 36, no. 17, pp. 3404–3406, 2011.

[14] B. Redding, M. A. Choma, and H. Cao, "Speckle-free laser imaging using random laser illumination," *Nat. Photonics*, vol. 6, no. 6, pp. 355–359, 2012.

[15] M. Nixon, O. Katz, E. Small, et al., "Real-time wavefront shaping through scattering media by all-optical feedback," *Nat. Photonics*, vol. 7, no. 11, pp. 919–924, 2013.

[16] B. Redding, C. Alexander, X. Huang, et al., "Low spatial coherence electrically pumped semiconductor laser for speckle-free full-field imaging," *Proc. Natl. Acad. Sci. U. S. A.*, vol. 112, no. 5, pp. 1304–1309, 2015.

[17] B. H. Hokr, S. Morgan, J. N. Bixler, et al., "A narrow-band speckle-free light source via random Raman lasing," *J. Mod. Opt.*, vol. 63, no. 1, pp. 46–49, 2016.

[18] S. F. Liew, S. Knitter, S. Weiler, et al., "Intracavity frequency-doubled degenerate laser," *Opt. Lett.*, vol. 42, no. 3, pp. 411–414, Feb 2017.

[19] K. Kim, S. Bittner, Y. Zeng, S. F. Liew, Q. Wang, and H. Cao, "Electrically pumped semiconductor laser with low spatial coherence and directional emission," *Appl. Phys. Lett.*, vol. 115, no. 7, p. 071101, 2019.

[20] H. Cao, C. Ronen, S. Bittner, A. A. Friesem, and N. Davidson, "Complex lasers with controllable coherence," *Nat. Rev. Phys.*, vol. 1, no. 2, pp. 156–168, 2019.

[21] J. A. Arnaud, "Degenerate optical cavities," *Appl. Opt.*, vol. 8, no. 1, pp. 189–196, Jan 1969.

[22] M. Nixon, B. Redding, A. A. Friesem, H. Cao, and N. Davidson, "Efficient method for controlling the spatial coherence of a laser," *Opt. Lett.*, vol. 38, no. 19, pp. 3858–3861, Oct 2013.

[23] S. Roelandt, Y. Meuret, C. Gordon, V. Guy, P. Janssens, and H. Thienpont, "Standardized speckle measurement method matched to human speckle perception in laser projection systems," *Opt. Express*, vol. 20, no. 8, pp. 8770–8783, Apr 2012.

[24] J. A. Arnaud, "Degenerate optical cavities. II: Effect of misalignments," *Appl. Opt.*, vol. 8, no. 9, pp. 1909–1917, 1969.
[25] Note that since our detector has an integration time of 0.1 ns, it is not possible to measure the entire beating frequency spectrum (32 GHz bandwidth) of the DCL but a part of it (5 GHz range).
[26] S. Bittner, S. Guazzotti, Y. Zeng, et al., "Suppressing spatiotemporal lasing instabilities with wave-chaotic microcavities," *Science*, vol. 361, no. 6408, pp. 1225–1231, 2018.
[27] D. Rick, *Probability: Theory and Examples*, vol. 49, Cambridge, UK, Cambridge University Press, 2019.

Supplementary Material: The online version of this article offers supplementary material (https://doi.org/10.1515/nanoph-2020-0390).